

Electrochemistry of (μ -Oxo)bis[(phthalocyaninato)manganese(III)]. A Four-Electron ECE Reduction Mechanism

P. C. MINOR* and A. B. P. LEVER*

Received July 16, 1982

The title complex undergoes a one-electron oxidation to a presumed mixed-valence species and a four-electron reduction to two molecules of mononuclear (Pc^{3-}) Mn^{II} . A detailed electrochemical study of the reduction process reveals an ECE mechanism. A brief study of the electrochemistry of mononuclear (Pc^{2-}) $\text{Mn}^{\text{III}}\text{OH}$ is also presented. The presence of a M-O-M bond in the title complex evidently shifts the various redox processes occurring at the metal atom negatively by about 700 mV. In particular, a Mn(IV) state seems quite accessible.

The title compound is the end product of the oxygenation of manganese(II) phthalocyanine in pyridine.^{1,2} Its identity, with axially coordinated pyridine ((pyMnPc)₂O), has been confirmed by X-ray crystallography.³

This species reacts with oxygen, in dimethylacetamide, quantitatively to form the adduct $\text{MnPc}(\text{O}_2)_2$,² a reaction that apparently involves conversion of oxide to oxygen. In view of the importance of such a reaction in the elucidation of photosynthesis,⁴ redox information on this complex seemed highly desirable. Preliminary studies⁵ suggested unusual behavior, which prompted this detailed study.

In pyridine solution the system exhibits a one-electron oxidation at about +0.35 V (vs. SCE) and reduction with scission of the Mn-O-Mn bonds at about -0.9 V. The reduction is a four-electron process involving an ECE mechanism whose details are discussed. A range of electrochemical techniques, including cyclic voltammetry, differential pulse polarography, and controlled-potential studies was used to elucidate this system.

Experimental Section

(Pc^{2-}) $\text{Mn}^{\text{III}}\text{O}-\text{Mn}^{\text{III}}(\text{Pc}^{2-})$ (I)^{1,6} and $\text{HOMn}^{\text{III}}\text{Pc}$ (III)² were prepared by previously reported methods and dried at 100 °C under vacuum. The supporting electrolyte (tetraethylammonium perchlorate, TEAP, Eastman Kodak) was thrice recrystallized from filtered hot aqueous solutions and finally dried at 60 °C, under vacuum. Pyridine (Fisher, reagent grade) was shaken with and distilled from barium oxide (Anachemia, reagent grade). The middle 60% was retained for use. Dimethylacetamide (DMA, Matheson Coleman and Bell, Spectroquality) was shaken with anhydrous sodium sulfate, decanted, and distilled under vacuum. The middle 60% fraction was used.

Voltammetry was carried out in three-electrode cells containing two platinum-wire electrodes. In subsequent experiments, a platinum-disk working electrode and a Luggin capillary were used. The capillary was adjusted to minimize iR drop, and the positive current feedback from the PAR 179 coulometer I/E converter was adjusted to just below the point of oscillation. Two coulometric cells were employed, one with a concentric mesh platinum working electrode and platinum-coil auxiliary electrode separated by a frit in a cylindrical vessel and the other with a spherical cell containing a platinum coil or mercury pool electrode and a platinum wire auxiliary. Both included

quartz cuvettes to monitor the electronic spectra (with Varian Cary 14 or Perkin-Elmer Model PE 340 spectrometers) of electrochemically generated species. Several reference electrodes were used including a Sargeant 30080 SCE and a texturized Vycor fritted SCE. These were calibrated with the ferrocene/ferrocenium couple in pyridine.

Slow-scan studies employed a Princeton Applied Research PAR 174A polarographic analyzer, with a PAR 121 drop timer, for polarography of the reduction waves. Fast-scan voltammetry was generated on a PAR 175A universal programmer, which triggered a PAR 173 potentiostat. Current/voltage curves were monitored on a Houston 2002 X-Y recorder or a Tektronix Model 5103N storage oscilloscope. Coulometric potentials were generated by the PAR 173 potentiostat, and the currents were integrated with a PAR 179 coulometer. All potentials are referred to the SCE.

Results and Discussion

The binuclear species I is indefinitely stable in pure acid-free pyridine. Cyclic voltammetry provides rapid insight into the rather unusual electrochemistry of this species.

Between 0 and +0.5 V, the species exhibits a reversible couple centered at 0.35 V in pyridine and an irreversible couple at 0.25 V in DMF (Figure 1A). At this potential, net oxidation of the solution species occurs. As detailed below, a one-electron oxidation is involved, presumably to form, initially, (Pc^{2-}) $\text{Mn}^{\text{III}}\text{O}-\text{Mn}^{\text{IV}}(\text{Pc}^{2-})$ (II).⁷ We discuss specifically the pyridine solution data. Pyridine solutions scanned from 0 to -0.8 V show no electroactivity; similarly if solutions are scanned from +0.5 to -0.8 V, only the oxidation couple is seen (Figure 1).

Upon continuation of the negative scan to about -1.0 V, an intense reduction wave is seen at about -0.9 V (Figure 1B), with no accompanying oxidation wave (irreversible reduction). However, when the positive scan is continued, new oxidation features appear at -0.8 V (C) and at 0 V (D), at potentials where previously no waves were observed. Both these waves arise through the chemistry that occurs after reduction of the bulk species at -0.9 V and are reminiscent of the theoretical curves derived by Nicholson and Shain for an ECE process where both electron transfers, $E(1)$ and $E(2)$, are reversible, $E(2)$ is positive of $E(1)$, and k_f/a is large (see below).^{8,9} When the scan is continued negatively (Figure 1), the reduction waves corresponding to C and D now appear. If the scan is continued to -1.6 V, a second reversible pair of waves is seen. Continuous high-speed cyclic voltammograms exhibit four sets of quasi-reversible waves centered at +0.35 (A), +0.089 (D), -0.857 (C), and -1.45 V. With the exception of couple A, this steady-state voltammogram is very closely similar to that

(1) Elvidge, J. A.; Lever, A. B. P. *Proc. Chem. Soc., London* **1959**, 195-6.

(2) Lever, A. B. P.; Wilshire, J. P.; Quan, S. K. *J. Am. Chem. Soc.* **1980**, *102*, 3668-9; *Inorg. Chem.* **1981**, *20*, 761-8.

(3) Vogt, L. H.; Zalkin, A.; Templeton, D. H. *Inorg. Chem.* **1967**, *6*, 1725-30.

(4) Renger, G. Z. *Naturforsch., B* **1970**, *25B*, 966-71. Cheniae, G. M.; Martin, I. F. *Biochim. Biophys. Acta* **1971**, *253*, 167-81. Kok, B.; Cheniae, G. M. *Curr. Top. Bioenerg.* **1966**, *1*, 2-47. Diner, B. A.; Joliot, P. *Encycl. Plant Physiol., New Ser. Anorg. Chem., Org. Chem., Biochem., Biophys., Biol.* **1977**, *5*, 187-205.

(5) Wilshire, J. P. Ph.D. Thesis, York University, 1977.

(6) Rayner-Canham, G. W.; Lever, A. B. P. *Inorg. Nucl. Chem. Lett.* **1973**, *9*, 513-6.

(7) Myers, J. F.; Rayner-Canham, G. W.; Lever, A. B. P. *Inorg. Chem.* **1975**, *14*, 461-68 (this paper introduces the phthalocyanine nomenclature used in the present paper).

(8) Nicholson, R. S.; Shain, I. *Anal. Chem.* **1965**, *37*, 178-90.

(9) Nicholson, R. S.; Shain, I. *Anal. Chem.* **1965**, *37*, 190-95.

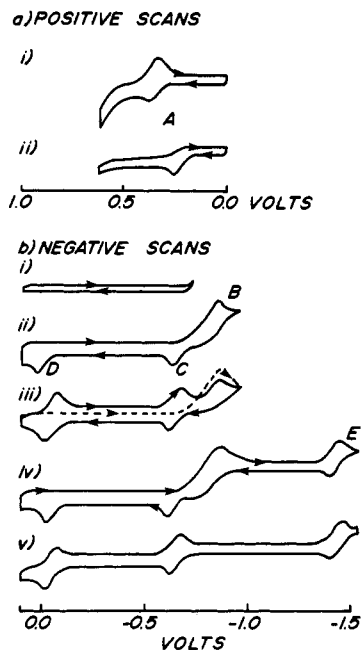


Figure 1. (a) Oxidation of species I in (i) pyridine, $E_{1/2} = 0.35$ V, and (ii) DMF, $E_{1/2} = 0.25$ V. (b) Reductive voltammograms of species I in pyridine: (i) initial scan +0.1 to -0.8 V; (ii) initial scan +0.1 to -1.1 V; (iii) initial (---) and second (—) scans +0.1 to -1.1 V; (iv) initial scan +0.1 to -1.6 V; (v) continuous scan 0.0 to -1.6 V. ($v = 0.1$ V/s except for (v) $v = 10.0$ V/s). TEAP is the innocuous electrolyte.

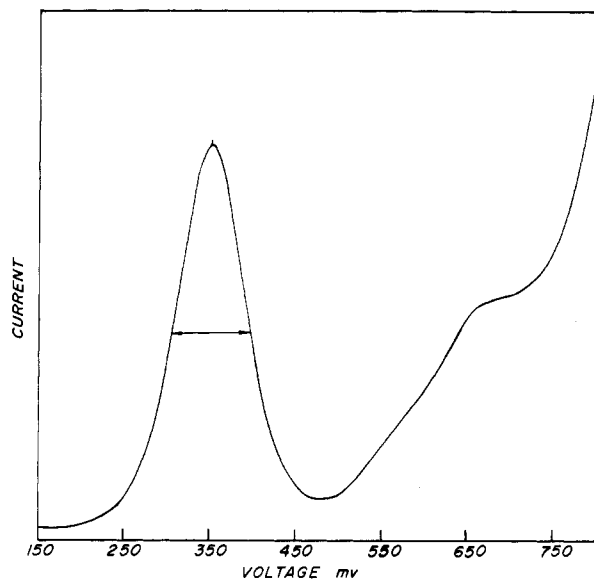


Figure 2. Differential pulse polarography of species I in pyridine/TEAP (scan rate 2 mV/s, $\Delta E = 5$ mV p-p).

obtained with mononuclear PcMn^{II} .¹⁰ We now discuss each wave in turn.

Oxidation Couple A. Cyclic voltammetry of the species I in pyridine at platinum-wire electrodes revealed one couple at 0.35 V. Peak separation (ΔE_p) for scans between 0.01 and 1.0 V/s are within 10 mV of ideality (59 mV) for a reversible one-electron oxidation. Peak current ratios (i_a/i_c) are within 10% of unity; neither cathodic nor anodic peaks shift markedly at these scan rates, indicating the insignificance of preceding or following coupled chemical reactions. Wave shape parameters, $E_p - E_{p/2}$ and $E_{1/2} - E_{p/2}$, lie within a few millivolts

Table I. Current/Voltage Parameters for the Oxidation of Species I in Pyridine

v , V/s	i_p , μA	$i_p/v^{1/2}$, $\mu\text{A}/(\text{V/s})^{1/2}$	i_c/i_d^a	i_c/i_d^b
0.001	0.62	19.6	1.68	1.65
0.002	0.72	16.1	1.38	1.35
0.005	1.00	14.1	1.21	1.16
0.010	1.33	13.3	1.14	1.09
0.020	1.84	13.0	1.11	1.04
0.050	2.70	12.1	1.03	1
0.100	3.70	11.7	1	1
0.200	5.25	11.7	1	1
0.500	8.15	11.5	1	1

^a Based on $i_d/v^{1/2} = 11.7 \mu\text{A}/(\text{V/s})^{1/2}$. ^b Calculated from Tables I and XII and Figure 14 of ref 13 with $k_f = 0.04 \text{ s}^{-1}$.

Table II. Voltammetric Data for Species I (1.7×10^{-4} M) in Pyridine/TEAP at a Pt-Disk Electrode (0.5-cm Diameter)

v , V/s	oxidn wave ^a			redn wave ^b	
	i , μA	$i_p/v^{1/2}$, $\mu\text{A}/(\text{V/s})^{1/2}$	i , μA	$i_p/v^{1/2}$, $\mu\text{A}/(\text{V/s})^{1/2}$	i_k/i_d^c
0.010	0.50	5.00	2.34	23.4	2.01
0.020	0.75	5.30	3.13	22.1	1.89
0.050	1.10	4.92	4.38	19.6	1.68
0.100	1.55	4.90	5.37	17.0	1.46
0.200	2.20	4.92	6.62	14.8	1.27
0.500	3.35	4.74	9.62	13.6	1.17
1.000	4.8				

^a At 0.353 V. ^b At -0.85 V. ^c See text for definition.

of their nominal values (57 and 28.5 mV, respectively) for a reversible reaction. Similarly a differential pulse voltammogram (Figure 2) yields a peak potential of 0.35 V and $W_{1/2}$ is 96 mV. All of the above are consistent with a reversible one-electron oxidation at the scan rates indicated. Above 1.0 V/s ΔE_p increases markedly probably because electron transfer is kinetically controlled (quasi-reversible).

However, under controlled-potential oxidation conditions at 0.45 V, the electrolysis current fails to decay to its background value with time, and the electronic spectrum of species I remains unaltered (under dry nitrogen or dry oxygen atmosphere).¹¹ Attempts to detect an oxidized species by electron spin resonance at ambient and low temperature also failed (species I is ESR silent). These two sets of observations seem consistent only with the suggestion of a slow catalytic process,^{12,13} following oxidation, which returns the oxidized species to I. Such a process is likely oxidation of solvent (pyridine) by the presumed $\text{PcMn}^{\text{IV}}\text{-O-Mn}^{\text{III}}\text{Pc}^+$ (II) product of the oxidation of I (Nicholson and Shain¹² case VII). We must conclude that a scan rate of 0.01 V/s is still too fast to observe this process by voltammetry.

In pursuit of evidence for the catalytic process, voltammetric single-scan studies were extended to 0.001 V/s. Although Nicholson and Shain consider the voltammetric diagnostic criteria usable down to "a few millivolts per second",¹² others warn of peak current and wave shape variations caused by convective mass transport at low scan rates.¹⁴ In previous studies of PcMn^{II} and other phthalocyanine monomers, such variations were evident at scan rates less than 0.005 V/s, but in no case did the observed peak current vs. scan rate deviate

(11) This experiment was repeated many times under varying conditions (dry and wet oxygen and nitrogen atmosphere, etc.). In most cases, no net chemistry was observed. However, in a small number of irreproducible cases, the complex (I) decomposed to the mononuclear manganese(III) species $\text{PcMn}^{\text{III}}\text{ClO}_4$.

(12) Nicholson, R. S.; Shain, I. *Anal. Chem.* **1964**, *36*, 706-23.

(13) Bard, A. J.; Faulkner, L. R. Eds. "Electrochemical Methods"; Wiley: New York, 1980.

(14) Headridge, J. P. "Electrochemical Techniques for Inorganic Chemists"; Academic Press: New York, 1969.

(10) Minor, P. C.; Lever, A. B. P.; Wilshire, J. P. *Inorg. Chem.* **1981**, *20*, 2550-3.

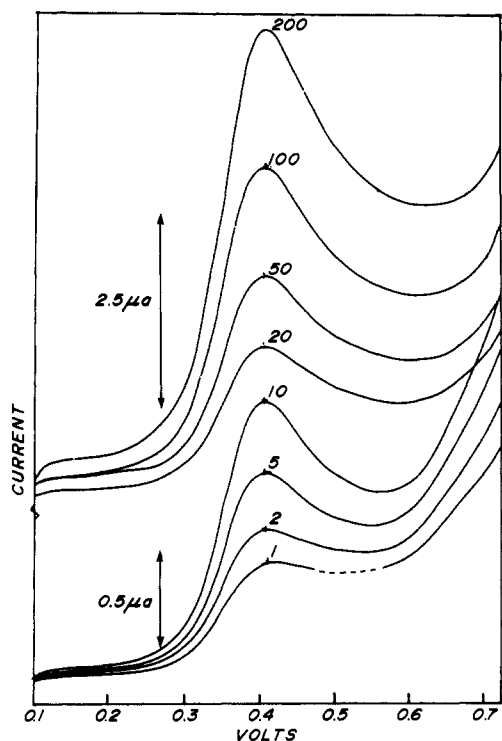
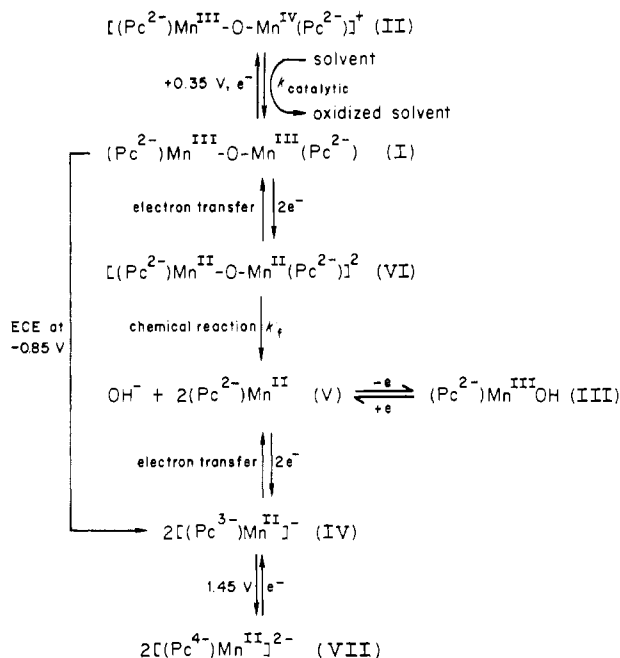


Figure 3. Single-scan voltammetry of species I in pyridine/TEAP (concentration of I = 4×10^{-4} M, Pt-disk electrode 0.5-cm diameter).

Scheme I



from expected Randles-Sevcik linearity by more than 10%. Given the structural similarity between monomeric and dimeric phthalocyanines, convection should affect solutions of each similarly. Table I shows the value of $i_p/v^{1/2}$ (v = scan rate) for the dimer oxidation, as a function of scan rate, based on current/voltage curves as shown in Figure 3. These curves mirror the experimental and calculated family of curves obtained by Saveant and Vianello¹⁵ for several catalytic systems. As expected for a catalytic system, the current parameter $i_p/v^{1/2}$ increases significantly at lower scan rates (<0.01 V/s). At scan rates above 0.01 V/s, the electron transfer is diffusion

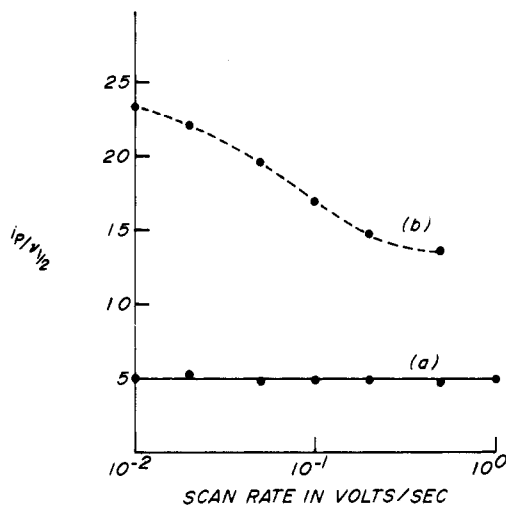


Figure 4. Comparison of oxidation (a) and reduction (b) peak currents $i_p/v^{1/2}$ vs. v (Pt-disk electrode 0.5-cm diameter, concentration of species I = 1.7×10^{-4} M).

controlled, while below 0.01 V/s the catalytic process becomes increasingly important with a limiting catalytic rate of $k_f \approx 0.04$ s⁻¹ based upon a working curve¹² of i_c/i_d vs. $(k_f/a)^{1/2}$, where $a = nFv/RT$. The experimental ratio $i(\text{catalytic})/i(\text{diffusion})$ is compared with the theoretical ratio in Table I. The agreement is good. Despite the expected convective errors, we tentatively conclude that the oxidation product $\text{PcMn}^{\text{IV}}\text{-O-Mn}^{\text{III}}\text{Pc}^+$ (II) catalytically oxidizes pyridine.

Because of the instability of species I in other solvents such as Me_2SO and DMF ,² we have been unable to study species I in other solvents. We anticipate further studies in the future, especially to seek the oxidation products of this reaction, which presents some unusual features that still await clarification.

Reduction Waves. Complex I is irreversibly reduced at about -0.85 V in py/TEAP. No return oxidation wave associated with this reduction is seen in the cyclic voltammogram. Controlled-potential reduction requires four electrons per dimer unit and generates a species characterized by its electronic spectrum as $(\text{py})_2\text{Mn}^{\text{II}}(\text{Pc}^{3-})$ (IV).¹⁶ The same mononuclear species is obtained through reduction of $\text{Mn}^{\text{II}}(\text{Pc}^{2-})$ (V) at about -0.8 V.¹⁰ Thus complex I undergoes scission upon reduction, thereby accounting for the irreversibility of wave B (Figure 1).

Since mononuclear IV is formed at the electrode, a positive return scan reveals band C, which corresponds to reoxidation of IV to $\text{Mn}^{\text{II}}(\text{Pc}^{2-})$ (V). There now exists mononuclear V in the diffusion layer, accounting for couple D, which arises from the mononuclear $\text{Mn}(\text{III})/\text{Mn}(\text{II})$ redox of V. The wave at about -1.45 V corresponds to formation of the doubly reduced mononuclear species $(\text{MnPc}^{3-})^{2-}$ (VII).¹⁵ The chemistry may be represented by Scheme I, where coordinated pyridine is omitted for clarity.

This reaction is characterized electrochemically as an ECE reaction (electron transfer, $E(1)$, followed by an irreversible chemical reaction, followed by a second electron transfer, $E(2)$). Its key electrochemical features are as follows: (i) $i_p/v^{1/2}$ is not constant and decreases with increasing scan rate (Figure 4); (ii) at low scan rates the chemical reaction is significant and thus the reduction peak current reflects both electron transfers, viz⁸

$$i_p = i_k = (-2.69 \times 10^5)(n_1 + n_2)(n_1)^{1/2}ACD^{1/2}v^{1/2} \quad (1)$$

where n_1 is the number of electrons involved in the first electron transfer and n_2 is the number involved in the second electron

(15) Saveant, J. M.; Vianello, E. *Electrochim. Acta* 1965, 10, 905-20.

(16) Clack, D. W.; Yandle, J. R. *Inorg. Chem.* 1972, 11, 1738-42.

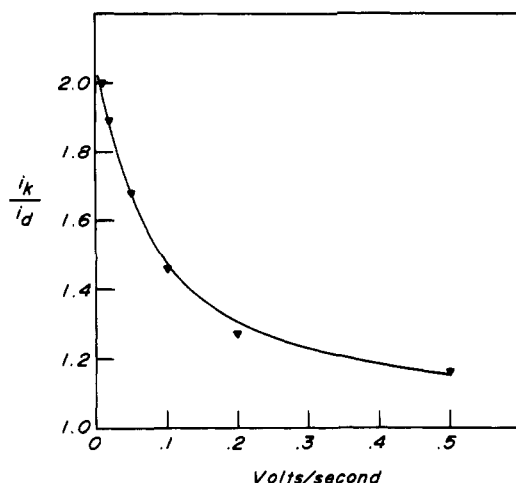


Figure 5. Plot of the function (3) in the form i_k/i_d vs. scan rate, with the assumption $k_f = 3.6 \text{ s}^{-1}$, for species I in pyridine/TEAP. Triangles indicate experimental values.

transfer, D is the diffusion coefficient, A is the electrode area, v is the scan rate, and C is the concentration. Controlled-potential coulometry shows that $n_1 + n_2 = 4$. At high scan rates the following chemical reaction and second electron transfer do not have time to occur and, therefore, the peak current reflects only the first electron transfer, viz. (Randles-Sevcik)^{13,17}

$$i_{p_r} = (-2.69 \times 10^5)(n_1)^{3/2}ACD^{1/2}v^{1/2} \quad (2)$$

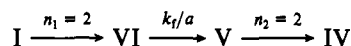
Since the oxidation current, i_{p_o} (at 0.352 V), at scan rates of 0.1 V/s or above is also given by the Randles-Sevcik equation, with the same values of the diffusion coefficient, electrode area, and bulk concentration,¹⁸ the ratio of these currents can provide values of n_1 and n_2 . Note that the data we have presented so far do not distinguish the three possibilities that scission may occur after the addition of one electron to form $(\text{Pc}^{2-})\text{Mn}^{\text{II}}\text{-O-Mn}^{\text{III}}(\text{Pc}^{2-})$ ($n_1 = 1, n_2 = 3$), after two electrons to form $(\text{Pc}^{2-})\text{Mn}^{\text{II}}\text{-O-Mn}^{\text{II}}(\text{Pc}^{2-})$ ($n_1 = 2, n_2 = 2$), or less probably, after three electrons to form $(\text{Pc}^{3-})\text{Mn}^{\text{II}}\text{-O-Mn}^{\text{II}}(\text{Pc}^{2-})$ ($n_1 = 3, n_2 = 1$). Therefore, at limiting low scan rates

	$n_1 = 1,$ $n_2 = 3$	$n_1 = 2,$ $n_2 = 2$	$n_1 = 3,$ $n_2 = 1$
i_{p_r}/i_{p_o}	4	5.7	6.9

where $n_0 = 1$, while at high limiting scan rates

	$n_1 = 1$	$n_1 = 2$	$n_1 = 3$
i_{p_r}/i_{p_o}	1	2.8	5.2

Our data with dilute solutions (ca. $1.7 \times 10^{-4} \text{ M}$) at 10 and 500 mV/s yields ratios of 5.6 and 2.4, respectively, for low and high scan rates.¹⁷ The data most closely correspond with $n_1 = n_2 = 2$. We propose that scission occurs after the addition of two electrons to form $(\text{Pc}^{2-})\text{Mn}^{\text{II}}\text{-O-Mn}^{\text{II}}(\text{Pc}^{2-})$. With neglect of the fate of the oxide ion, which probably reacts with expeditious protons to yield hydroxide, the reaction may be represented

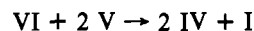


The rate constant for the chemical reaction can be estimated from⁹

$$i_k/i_d = (0.4 + k_f/a)/(0.396 + 0.469k_f/a) \quad (3)$$

i_k is the observed peak current at scan rate v , when the chemical reaction is important, and i_d is the diffusion current

at the same sweep rate in the absence of the following reaction. This latter term can be estimated from the limiting value of the $i_p/v^{1/2}$ curve, at high scan rate. A value of $k_f \approx 3.6 \text{ s}^{-1}$ is obtained in this fashion. This can only be a rough estimate, obtained in dilute solution, because a further reaction, which becomes important in more concentrated solutions, must be considered. The initial reaction product following electron transfer, $E(1)$, namely, $(\text{Pc}^{2-})\text{Mn}^{\text{II}}\text{-O-Mn}^{\text{II}}(\text{Pc}^{2-})$ (VI), has sufficient potential to reduce $(\text{Pc}^{2-})\text{Mn}^{\text{II}}$ since the following electron transfer, $E(2)$, occurs at a potential positive of $E(1)$. Thus a complicating secondary reaction in the vicinity of the electrode will be



This is a kind of disproportionation reaction between product and reactant.¹⁹ It should lead to a greater than anticipated current at higher concentrations since it will proceed faster than the electrode reaction, causing a renewal of the unreduced μ -oxo species (I) at the electrode. Indeed, in solutions exceeding 10^{-4} M , the observed current i_d/i_k at low scan rates is greater than provided for by the theory outlined above unless this disproportionation reaction is included.

In summary, the binuclear complex I is significantly more stable toward reduction than mononuclear $\text{Mn}^{\text{III}}(\text{Pc}^{2-})$, which is reduced near 0 V.¹⁰ After a two-electron reduction at -0.9 V , a dimeric manganese(II) species, VI, is presumably formed. This undergoes scission with $k_f \approx 3.6 \text{ s}^{-1}$, generating mononuclear $(\text{Pc}^{2-})\text{Mn}^{\text{II}}$ (V), which is now poised at a potential about 0.1 V more negative than that for its reduction to $\text{Mn}^{\text{II}}(\text{Pc}^{3-})$ (IV). Thus an additional 2 e/binuclear unit is provided to effect reduction to IV.

Below -0.9 V , mononuclear IV is generated at the electrode and at -1.4 V we see its reduction to the doubly reduced mononuclear VII. The relative peak intensities at -0.9 and -1.45 V are approximately 2:1 as anticipated for this mechanism.

Hydroxy(phthalocyaninato)manganese(III). The chemistry outlined above is clearly due to the presence of two closely lying phthalocyanine rings; however, it is useful to question the role of axially bound oxygen in modifying MnPc potentials. We, therefore, consider here the voltammetry of $(\text{Pc}^{2-})\text{Mn}^{\text{III}}\text{OH}$. The almost diamagnetic spin-coupled PcMn-O-MnPc is susceptible to cleavage by nucleophiles such as hydroxide, chloride, and water.² Thus the high-spin hydroxy complex III is readily prepared by treating a solution of the binuclear complex I with a small amount of water. Its voltammetry (below) is typical of a $\text{XMn}^{\text{III}}\text{Pc}$ species with strongly bound X.

In porphyrin chemistry there has previously been confusion over species formulated as $\text{PM}(\text{OH})$ because of the difficulty in distinguishing between the hydroxo, aquo, and oxo-bridged structural possibilities. Such a problem does not arise here. The oxo-bridged system, namely, I, is known and spectroscopically distinct from III, and a possible formulation for III, $(\text{H}_2\text{O})\text{Mn}^{\text{III}}(\text{Pc}^{2-})^+\text{OH}^-$, is ruled out, both by analysis and by voltammetry (below). The water molecule in such a species would surely be replaced by solvent. We do not observe an O-H stretching vibration in the infrared spectrum of this complex, but this is not uncommon for such a massive HOMnPc species.²⁰

A cyclic voltammogram of III in py/TEAP reveals that the potentials for the Mn(III)/Mn(II) couple and for the two successive reduction couples to $(\text{MnPc})^-$ and $(\text{MnPc})^{2-}$ are

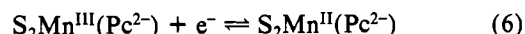
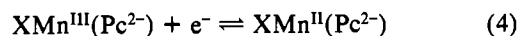
(17) Sevcik, A. *Collect. Czech. Chem. Commun.* **1948**, *13*, 349-77. Randles, E. B. *Trans. Faraday Soc.* **1948**, *44*, 327-38.

(18) So that the current due to the catalytic process in the oxidation wave (at $+0.35 \text{ V}$) could be eliminated, the diffusion current at 0.01 V/s appropriate for the oxidation wave was calculated from the reversible charge transfer $i_p/v^{1/2}$ value of $11.7 \mu\text{A}/(\text{V/s})^{1/2}$.

(19) Mastragostino, M.; Nadjio, J. M.; Saveant, M. *Electrochim. Acta* **1968**, *13*, 721-49.

(20) Elvidge, J. A.; Lever, A. B. P. *J. Chem. Soc.* **1961**, 1257-1265.

essentially identical, as anticipated, with the previously described voltammetry of $\text{Mn}^{\text{II}}\text{Pc}$ in py/TEAP.¹⁰ However, there are two distinguishing features. At fairly high scan speeds, a new reduction peak, A', is associated with the Mn(III)/Mn(II) couple, on the negative side of the reduction wave, A. The total current is shared between A and A', with A' being more prominent at high scan speeds and being absent at low scan speeds (0.1 V/s). By analogy with the $\text{Mn}^{\text{II}}\text{Pc}/\text{DMA}/\text{Cl}$ system, this behavior is readily interpreted in terms of the equilibria given by eq 4-7. We can confidently expect that



the potential of couple 4 will be more negative than that of couple 6. At slow speeds, with scans going negatively from the potential of the resting solution (zero current, $0.8 > v > -0.03$ V), there is time for the bulk species III to dissociate according to the right-hand side of (7), and then to be reduced (wave A) according to (6). At high scan speeds there is insufficient time for equilibrium (7) to shift to the right, and the hydroxo species III is directly reduced to VIII according to reaction 4. The reduced hydroxo species VIII has a very short lifetime (5), and no oxidation of this species is observed, even at very high scan speeds.

There is an irreversible wave, B, which occurs near +0.8 V and probably corresponds to oxidation of the ligand since it is observed 1.6 V from ligand reduction.²¹ Oxidation to Mn(IV) must, therefore, be at least as anodic as +0.8 V. There is no accompanying reduction wave, and it is reasonable to assume that oxidation of the solvent occurs rapidly. The $\text{Mn}^{\text{II}}\text{Pc}/\text{py}/\text{TEAP}$ system does not oxidize below the solvent limit.

Conclusions

We have completed an electrochemical study of $\text{Mn}^{\text{II}}\text{Pc}$ (V), $\text{HOMn}^{\text{III}}\text{Pc}$ (III), and $\text{PcMn}^{\text{III}}\text{O}-\text{Mn}^{\text{III}}\text{Pc}$ (I). Most significant is the observation that the Mn(IV)/Mn(III) couple shifts negatively in the sequence



and, indeed, in the binuclear complex I, the +IV state is readily accessible, if reactive. Moreover, in the binuclear species I, the Mn(III)/Mn(II) couple shifts about 0.7 V negatively; i.e., the +III state becomes very much more stable than in the mononuclear species. This latter chemistry is very similar to that of $(\text{TPP})\text{Fe}^{\text{III}}\text{O}-\text{Fe}^{\text{III}}(\text{TPP})$, which shows its initial reduction at -0.93 V, compared with -0.2 V for the mononuclear species. The binuclear iron system cleaves after it has been reduced by one electron to $(\text{TPP})\text{Fe}^{\text{II}}\text{O}-\text{Fe}^{\text{III}}(\text{TPP})$, picking up three more electrons to form $\text{Fe}^{\text{I}}(\text{TPP})$. In this case, the initial one-electron mixed-valence reduction product may be identified, by ESR, at 70 K. Kadish and co-workers²² also note formation of $\text{HOFe}^{\text{II}}(\text{TPP})$, which is about 0.35 V more stable toward reduction than $\text{Fe}^{\text{II}}(\text{TPP})$. Similarly the one-electron oxidation of $(\text{TPP})\text{Fe}^{\text{III}}\text{O}-\text{Fe}^{\text{III}}(\text{TPP})$ is negatively shifted about 300 mV relative to that for $(\text{TPP})\text{Fe}^{\text{III}}\text{Cl}$.²³ The presence of two phthalocyanine or porphyrin rings in close proximity (about 360 pm apart) has a significant effect upon electronic spectrum, implying interaction between the rings. Possibly electron donation from both rings serves to favor the high oxidation states. However, note that very similar behavior is also observed with the $[\text{Fe}(\text{Salen})]_2\text{O}$, $\text{Fe}(\text{Salen})$, and $\text{HOFe}(\text{Salen})$ complexes.²⁴

These systems provide a possible archetypical mechanism for biological oxidation. The mixed-valence binuclear molecule containing M(IV) can readily be formed under mildly oxidizing conditions yet, upon cleavage or dissociation, generates a very powerful oxidizing agent, the mononuclear M(IV) species,²⁵ which will have a potential of at least +0.8 V. Further studies of the redox possibilities of this system, with various organic substrates, are in hand.

Acknowledgment. This project was initiated by Dr. J. P. Wilshire, to whom we are indebted for early discussions. The research is part of a joint project with Professor A. J. Bard (University of Texas at Austin) funded by the Office of Naval Research, to whom we are also indebted. Funds from the Natural Sciences and Engineering Research Council (Ottawa, Canada) are also appreciated.

Registry No. I, 12581-72-5; II, 84174-26-5; III, 63105-50-0.

(21) Lever, A. B. P.; Minor, P. C. *Inorg. Chem.* **1981**, *20*, 4015-17.

(22) Kadish, K. M.; Larson, G.; Lexa, D.; Momenteau, M. *J. Am. Chem. Soc.* **1975**, *97*, 282-88.
 (23) Kadish, K. M.; Cheng, J. S.; Cohen, I. A.; Summerville, D. "Electrochemical Studies of Biological Systems"; American Chemical Society: Washington, DC, 1977; ACS Symp. Ser. No. 38, pp 65-77.
 (24) Wenk, S. E.; Schultz, F. A. *J. Electroanal. Chem. Interfacial Electrochem.* **1979**, *101*, 89-99
 (25) Chin, D.-H.; Balch, A. L.; La Mar, G. N. *J. Am. Chem. Soc.* **1980**, *102*, 1447-8.